第33卷 第5期 焊 接 学 报 Vol. 33 No. 5
2012年5月 TRANSACTIONS OF THE CHINA WELDING INSTITUTION May 2012

2A97铝锂合金搅拌摩擦焊

张 华[1,3]， 孔德跃[2]， 陈雪峰[2]， 曹 健[3]， 赵衍华[2]， 黄继华[1]
（1. 北京科技大学 材料科学与工程学院，北京 100083；2. 首都航天机械公司，北京 100076；
3. 哈尔滨工业大学 先进焊接与连接国家重点实验室，哈尔滨 150001）

张 华

摘 要：文中采用不同搅拌摩擦焊接工艺参数对2A97铝锂合金的可焊性进行了研究. 结果显示，接头抗拉强度和断后伸长率随搅拌头转速的提高而降低，随焊接速度的提高先增后减. 在旋转频率为600 r/min，焊接速度200 mm/min时接头抗拉强度最高达到373 MPa，为母材的69%. FSW接头拉伸试验断口位置基本都发生在焊核(NZ)区. 焊核区和热力影响区中沉淀相大部分溶解，只有少数存留，热力影响区沉淀相密度高于焊核区.

关键词：铝锂合金；搅拌摩擦焊；微观组织；力学性能
中图分类号：TG453.9 **文献标识码**：A **文章编号**：0253－360X(2012)05－0041－04

0 序 言

铝锂合金是一种低密度、高性能的新型结构材料，随着航空航天工业的迅猛发展，铝锂合金也得到了日益广泛的应用，用铝锂合金取代常规的铝合金可使结构质量减轻10%～15%，刚度提高15%～20%. 用2195铝锂合金作为航天飞机外箱的材料，结构质量比原来采用2219材料减轻7%，有效载荷增加10%～15%. 随着Al-Li合金在航空航天业中的广泛应用，其焊接性的研究日益受到了重视[1]. 使用传统的焊接工艺如气体钨极电弧焊、气体金属电弧焊和等离子弧焊，焊缝及近缝区易出现焊接气孔和裂纹等缺陷[2-6]，使焊接区力学性能下降，因而采用更加科学的焊接方法，减少贮箱焊接过程缺陷的产生，成为亟待解决的关键的科学技术及工程实际问题.

搅拌摩擦焊是一种新的连接方法，通过高速旋转的搅拌头与被焊材料表面间生成的摩擦热而实现的固相连接，适用于高强铝锂合金等航空材料的焊接，并已在铝合金焊接方面取得巨大的成功[7-9]. 搅拌头的旋转搅拌作用可有效破碎待焊表面的氧化膜，因而焊前不需预处理，从而解决了铝锂合金表面氧化膜给焊接过程带来的困难，并简化了焊接工艺，节约了成本. 采用搅拌摩擦焊工艺连接铝锂合金焊接温度低，材料没有发生熔化，因而避免了合金中Li元素的挥发损失、接头内不易形成脆性相和热裂纹、接头残余应力低、强度系数高[10]. 文中以2A97铝锂合金为母材，研究搅拌摩擦工艺对接头成形及力学性能的影响.

收稿日期：2011－12－30
基金项目：国家自然科学基金资助项目(51105030)；哈尔滨工业大学先进焊接与连接国家重点实验室资助项目(AWPT-M06)；中央高校基本科研业务费专项资金资助

1 试验材料与FSW接头制备

论文试验所采用的材料为2A97铝锂合金. 试验采用1.9 mm厚2A97铝锂合金板材，状态为T8. 其化学成分和力学性能分别见表1和表2. 可以看出，合金中铜、锂含量较高，铜和锂在合金中形成主要的强化相.

表1 2A97铝锂合金化学成分(质量分数，%)
Table 1 Compositions of 2A97 Al-Li alloy

Cu	Mg	Li	Zr	Ag	Fe	Si	Zn	Al
4.2	0.4	1.2	0.1	0.3	0.15	0.2	2.05	余量

表2 2A97铝锂合金力学性能
Table 2 Mechanical properties of 2A97 Al-Li alloy

屈服强度 R_{eL}/MPa	抗拉强度 R_m/MPa	断后伸长率 A(%)	显微硬度 HV
≥455	≥520	≥6	215

铝锂合金焊前为轧制状态，微观形貌为沿轧制方向的带状组织，带状组织内存在2～2.5 μm的亚

晶组织，如图 1 所示. 合金内含有 T1(Al2CuLi) 和 β'(Al3Zr) 沉淀相，其中 T1 相是合金内的主要强化相，少量的 β'沉淀弥散分布于晶内. T1 相是平衡相，呈六角薄片状或针状，长 50 nm，厚 1 nm，属于六方晶系($a=0.497$ nm，$c=0.934$ nm) . β'为亚稳相，呈球状，具有 Ll2 型有序结构，点阵常数为 0. 408 nm. β'相可有效钉扎晶界和亚晶界，起到阻碍再结晶和细化晶粒的作用.

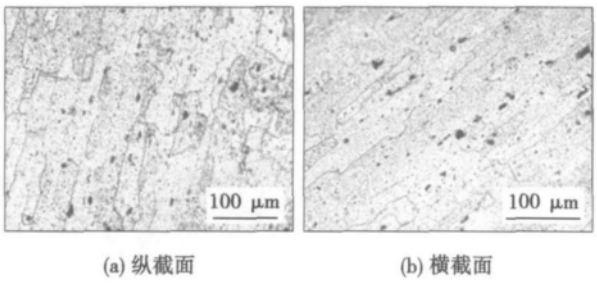

图 1 2A97 铝锂合金母材组织形貌

Fig. 1 Microstructure of 2A97 Al-Li alloy

文中 2A97 铝锂合金 FSW 焊接工艺参数选择强规范，参数如表 3 所示. 不同焊接工艺参数下，焊缝表面光洁度不同. 其粗糙程度受焊接参数的影响，随着焊接速度的增加或转速的降低，焊缝表面渣状物越来越少，金属光泽越明显，表面成形越美观. 为方便描述，定义旋转频率与焊速的比值为 m.

表 3 试样焊接参数

Table 3 FSW parameters of samples

编号	转转频率 n/(r·min^{-1})	焊接速度 v/(mm·min^{-1})	旋转频率/焊接速度比值 m/(r·mm^{-1})	抗拉强度 R_m/MPa
1	600	200	3	373.24
2	800	200	4	334.85
3	1 000	100	10	344.64
4	1 000	150	6.7	357.51
5	1 000	200	5	315.19
6	1 000	250	4	331.49
7	1 200	200	6	313.66
8	1 400	200	7	275.19

2 FSW 接头力学性能

搅拌摩擦焊接 2A97 铝锂合金的强度最高可达母材 69%，最低则只有 51%(表 3) . 接头的断后伸长率较母材相比下降比较多. 试样基本都断在焊核区，说明该区域是这类焊接接头的最薄弱部位.

2.1 焊接速度对接头力学性能的影响

图 2 为焊接速度对 2A97 铝锂合金搅拌摩擦焊接头抗拉强度的影响. 随着焊接速度的提高，抗拉强度先增后减. 当焊接速度小于 150 mm/min 时，抗拉强度随焊接速度的提高而增大，在焊接速度为 150 mm/min 时达到最大值 357. 51 MPa; 当焊接速度大于 150 mm/min 时，接头抗拉强度随焊接速度的提高而迅速降低.

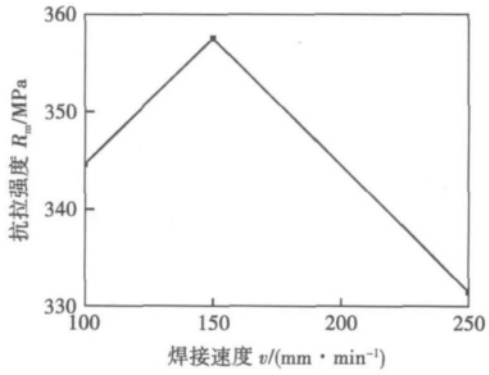

图 2 焊接速度对接头抗拉强度的影响(v=1 000 r/min)

Fig. 2 Effect of welding speed on tensile strength

2.2 搅拌头旋转频率对接头力学性能的影响

图 3 为旋转频率对 2A97 铝锂合金搅拌摩擦焊接头抗拉强度的影响. 当旋转频率增加时，接头抗拉强度降低. 当旋转频率大于 1 200 r/min 时，抗拉强度下降幅度迅速增大. 强度下降的原因应是热输入量过大，导致弱区软化严重，强度降低.

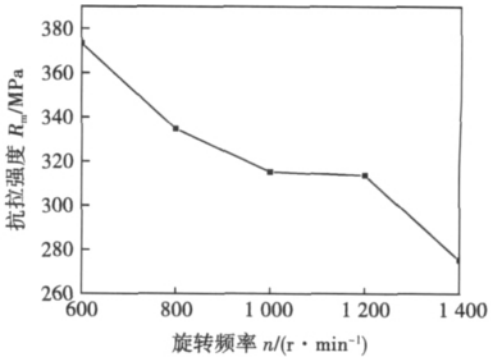

图 3 旋转频率对接头抗拉强度的影响 (v=200 mm/min)

Fig. 3 Effect of rotation speed on tensile strength

2.3 旋转频率/焊接速度对接头力学性能的影响

图 4 为旋转频率/焊接速度比值与抗拉强度的关系. 当 m 同为 4 r/mm 时，抗拉强度为 334. 85 MPa 与 331. 49 MPa，表明 m 相同时，抗拉强度与断后伸长率基本相同(表 3) . 抗拉强度在 m 为 3 r/mm 时最大，而在 7 r/mm 时最小. 除了 1 号焊件断在轴肩上外，其余的焊件皆在焊缝中心发生断裂. 断

口为韧脆混合断裂,但主要以脆断为主.

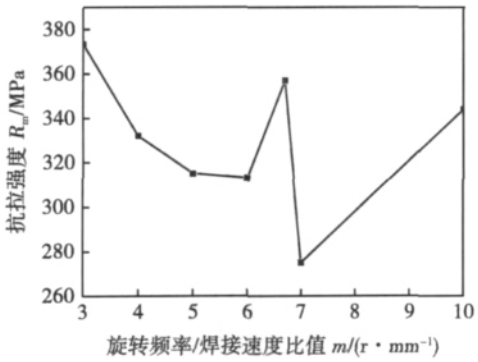

图 4　旋转频率/焊接速度比值对接头抗拉强度的影响 (v =200 mm/min)

Fig. 4　Effect of heat input on tensile strength of joints

3　FSW 接头微观组织

3.1　焊缝横截面形貌

图 5 为 2A97FSW 接头横截面组织. 从图 5 中可以看出,接头可分为四个区域,焊缝中部的焊核区(NZ) 、热力影响区(TMAZ) 、热影响区(HAZ) 以及母材(BM) . 焊缝整体与搅拌针形状相似,但不对称,焊缝在后退侧所占比例较大,且前进侧边界比较清晰,而后退侧边界则比较模糊. 这主要是因为焊接过程中后退侧的热量较大,塑性化材料较多,热变形区域较大. 前进侧则在焊接过程中受搅拌针剪切作用较大,该部分材料应变梯度较大,故界限比较清晰. 但随着热量的增加,两侧逐渐开始变得对称,前进侧边界也开始变得模糊.

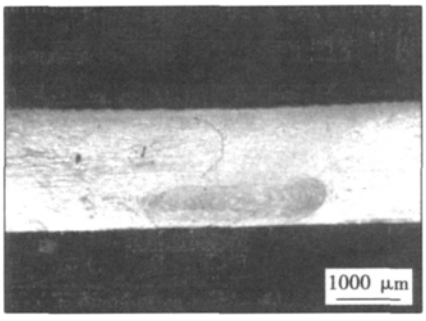

图 5　2A97FSW 接头横截面典型组织

Fig. 5　Microstructure of 2A97 FSW joint

3.2　焊核区

焊核区金属在搅拌头强烈搅拌摩擦作用下发生显著的塑性变形,形成了细小、均匀的晶粒,并且沉淀相的数量较其它各区明显增加,晶界较难分辨(图 6) . 由于铝合金的层错能较高,很难发生断续动态再结晶(DDRX) ,因而,铝合金在热变形时主要发生连续动态再结晶(CDRX) ,其发生再结晶的机制主要为亚晶转变为晶粒,而位错不断进入亚晶界是亚晶界取向角不断增大转变为大角晶界的主要机制.

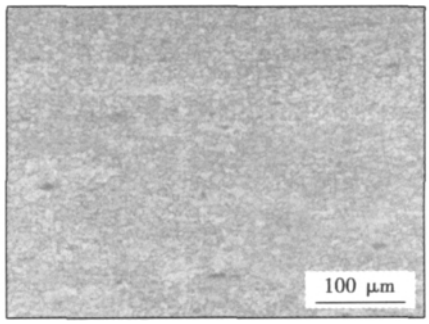

图 6　焊核区组织 (n =1 400 r/min, v =200 mm/min)

Fig. 6　Microstructure of weld nugget in 2A97 FSW joint

3.3　热力影响区

图 7 为前进面热力影响区(TMAZ) 金相组织形貌. 该区金属在搅拌头的热力作用下发生不同程度的塑性变形和部分再结晶,同时,热力影响区的组织在搅拌摩擦焊接过程中发生弯曲变形,与母材的原始组织取向呈一定的角度; 热力影响区的晶粒受到热和机械的共同作用,晶粒发生了机械变形,但由于温度和变形程度都低于焊核区,因此该区只有部分晶粒发生了再结晶,大部分晶粒保持了变形后的形态.

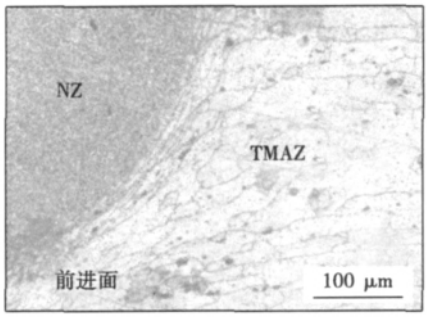

图 7　热力影响区组织 (n =1 000 r/min, v =250 mm/min)

Fig. 7　Microstructure of heat-mechanical affected zone

3.4　热影响区

在热力影响区以外的部分区域为热影响区,其与热力影响区没有明显分界线,该区金属没有受到搅拌头的机械搅拌作用,仅受到摩擦产热的影响,晶粒稍有长大,但与母材相比变化很小,见图 8.

3.5　显微硬度

图 9 为 2A97FSW 接头显微硬度. 从图 9 可以

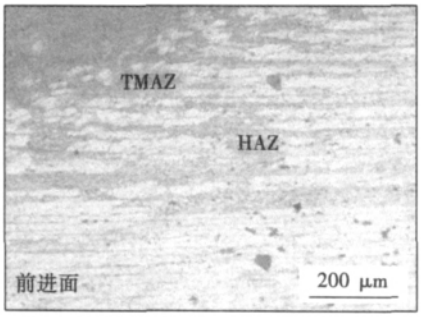

图 8 热影响区组织(n = 600 r/min, v = 200 mm/min)
Fig. 8 Microstructure of heat affected zone

看出焊缝两侧距焊缝中心一定距离的位置出现硬度明显降低的区域,且该区域的宽度和硬度值水平与焊接工艺参数有关. 焊核区微观硬度较高,热影响区微观硬度相对较低. 两种不同区域交界处,容易出现硬度突变. 显微硬度分布与沉淀相密切相关. 在热影响区,细小的强化相会发生聚集现象,因为在这个区域温度较低,导致产生过时效作用,使接头强度和显微硬度降低. 焊核区晶粒非常细小,微观硬度保持在一个较高的水平.

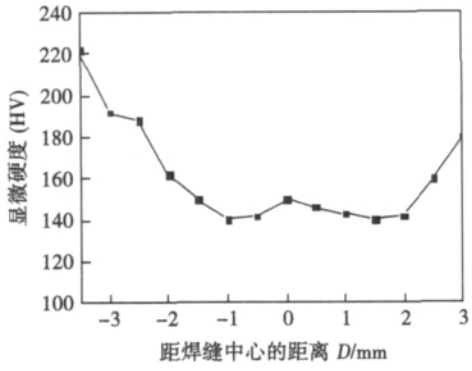

图 9 2A97FSW 搅拌摩擦焊接头显微硬度
Fig. 9 Microhardness of 2A97 FSW joint

4 结 论

(1) 2A97 铝锂合金 FSW 接头拉伸试验断裂基本都发生在焊核(NZ) 区,当旋转频率为 600 r/min,焊接速度为 200 mm/min 时断裂发生在轴肩位置.

(2) 接头抗拉强度随焊接旋转频率的提高而降低,随焊接速度的提高先增后减. 在旋转频率为 600 r/min,焊接速度 200 mm/min 时接头抗拉强度最高达到 373 MPa,为母材的 69%.

(3) 2A97 铝锂合金母材和焊缝拉伸断口呈韧脆混合断裂模式,但主要以脆性断裂为主.

(4) 焊核区和热力影响区中沉淀相大部分溶解,只有少数存留,但热力影响区沉淀密度高于焊核区.

参考文献:

[1] 霍红庆, 郝维新, 耿桂宏, 等. 航天轻型结构材料—铝锂合金的发展[J]. 真空与低温, 2005, 11(2): 63 - 69.
Huo Hongqing, Hao Weixin, Geng Guilong, *et al*. Development of the new aerocraft material: Aluminum-Lithium alloy [J]. Vacuum and Cryogenics, 2005, 11(2): 63 - 69.

[2] Solo´rzano I G, Darwish F A. Effect of weld metal microstructure on the monotonicand cyclic mechanical behavior of TIG welded 2091 Al-Li alloy joints [J]. Materials Science and Engineering A, 2003, 348: 251 - 261.

[3] 杨 璟, 李晓延, 巩水利, 等. 铝锂合金 YAG-MIG 复合焊焊缝成形特征[J]. 焊接学报, 2010, 31(2): 83 - 86.
Yang Jing, Li Xiaoyan, Gong Shuili, *et al*. Characteristics of aluminum-lithium alloy joint formed by YAG-MIG hybrid welding [J]. Transactions of the China Welding Institution, 2010, 31(2): 83 - 86.

[4] 庄 蕾, 罗 宇, 王亚军, 等. 1420 铝锂合金激光焊接工艺研究[J]. 焊接, 2006(1): 39 - 42.
Zhuang Lei, Luo Yu, Wang Yajun, *et al*. Study on laser welding of 1420 Al-Li alloy [J]. Welding & Joining, 2006(1): 39 - 42.

[5] Wang D Y, Feng J C, Wang P F. Friction stir welding of Al-Li alloy [J]. Materials Science and Engineering, 2005, 23(3): 369 - 372.

[6] 闫国永,李绍成. 铝锂合金无中间层扩散焊接工艺研究[J]. 材料开发与应用, 2001, 16(2): 10 - 12.
Yan Guoyong, Li Shaocheng. Research on diffusion welding technology of Al-Li alloys without interlayer [J]. Development and Application of Materials, 2001, 16(2): 10 - 12

[7] 张 华, 林三宝, 吴 林, 等. 搅拌摩擦焊研究进展及前景展望[J]. 焊接学报, 2003, 24(3): 91 - 96.
Zhang Hua, Lin Sanbao, Wu Lin, *et al*. Current progress and prospect of friction stir welding [J]. Transactions of the China Welding Institution, 2003, 24(3): 91 - 96

[8] 郭晓娟, 李 光, 董春林, 等. 1420 铝锂合金搅拌摩擦焊接力学性能[J]. 焊接学报, 2009, 30(4): 45 - 48
Guo Xiaojuan, Li Guang, Dong Chunlin, *et al*. Mechanical properties of 1420 aluminum-lithium alloy friction stir welding [J]. Transactions of the China Welding Institution, 2009, 30(4): 45 - 48

[9] Dawea C J, Thomas W M. Friction stir process welds aluminum alloys [J]. Welding Journal, 1996, 75(3): 41 - 45

[10] 王大勇, 冯吉才, 王攀峰. 铝锂合金搅拌摩擦焊研究[J]. 材料科学与工程学报, 2005, 23(3): 369 - 373.
Wang Dayong, Feng Jicai, Wang Panfeng. Friction stir welding of Al-Li alloy [J]. Journal of Materials Science & Engineering, 2005, 23(3): 369 - 373.

作者简介: 张 华,女,1976 年出生,博士,副教授. 主要从事搅拌摩擦焊方面的科研和教学工作. 发表论文 30 余篇. Email: zhhwhq@163.com

通讯作者: 黄继华,男,教授. Email: jihuahuang47@sina.com.

of Materials Science and Technology, Nanjing University of Aeronautics and Astronautics, Nanjing 210016, China; 2. Harbin Welding Institute, Harbin 150080, China; 3. Changshu Huayin Filler Metals Co., Ltd, Changshu 215513, China). pp 33 – 36

Abstract: Effects of rare earth element Pr additions on the microstructure and properties of Sn-Zn-Ga solder were studied in this paper. The wettability of solder was significantly improved by 0.08% Pr addition. However, the wettability of solder would deteriorate when the Pr addition exceeds 0.12% due to the oxidization of Pr element at the liquid surface. Moreover, the mechanical property of solder joint was improved by Pr addition and the maximum shear strength was obtained when 0.08% Pr was added. The Zn-rich phase in the solder matrix was refined by Pr but the thickness of interface layer showed no obvious difference when Pr was less than 0.08%. When excessive Pr was added, the interface layer thickness of the joint increased significantly, so that the optimal content of Pr in the Sn9Zn0.5Ga solder is about 0.08%.

Key words: Sn-Zn fill metal; wettability; mechanical properties; microstructure

Double-side friction stir welding of wear resistant aluminum silicon copper alloy ZHANG Zhiyun, CHEN Maoai, WU Chuansong (MOE Key Laboratory for Liquid-Solid Structural Evolution and Materials Processing, Shandong University, Jinan 250061, China). pp 37 – 40

Abstract: The 10 mm thick wear resistant Al-Si-Cu alloy plates were double-side friction stir welded (D-FSW). The microstructure and mechanical properties of the joints were investigated. The results show that the as-cast Al grain and Si reinforcement particles in the weld are remarkably refined during friction stir welding. The distribution of Si particles in the weld is more uniform than that in as-received base metal. The refinement of the grains and the uniformity of Si particles in the second pass are better than those in the first one. The joints of double pass welding in opposite direction (OD joints) exhibit lower tensile strength than those of double pass welding in the same direction (SD joints). All the OD joints fractured through the advancing side of the joints, while the fracture paths of SD joints depend on the welding parameters. The tensile strength of SD joints welding at a stirring tool rotating speed of 950 rpm and a welding speed of 10 mm·min^{-1} is up to 87.4% of the base metal.

Key words: double-side friction stir welding; Al-Si-Cu alloy; microstructure; grain refinement; tensile strength

Study on friction stir welding of 2A97 Al-Li alloy ZHANG Hua[1,3], KONG Deyue[2], CHEN Xuefeng[2], CAO Jian[3], ZHAO Yanhua[2], HUANG Jihua[1] (1. School of Materials Science and Technology, University of Science and Technology Beijing, Beijing 100083, China; 2. Capital Aerospace Machinery Company, Beijing 100076, China; 3. State Key Lab of Advanced Welding and Joining, Harbin Institute of Technology, Harbin 100051, China). pp 41 – 44

Abstract: The weldability of 2A97 Al-Li alloy was studied using different friction stir welding variables in this paper. The results showed that the tensile strength and the elongation rate decreased with the increasing of the rotation speed. With the increasing of the welding speed, the tensile strength firstly increased to a maximum value then decreased. The maximum tensile strength was 373 MPa, which reached to 69% of that of the base metal, when the rotation speed was 600 r/min and the welding speed was 200 mm/min. The joints were mostly fractured at the weld nugget. Most of the precipitated phases in the weld nugget and the heat affected zone were decomposed. The precipitate density in the heat affected zone was higher than that in the weld nugget.

Key words: Al-Li alloy; friction stir welding; microstructure; mechanical properties

Numerical simuation of welding residual deformation in welded joints of marine steel plate by FEM LU Xuedong[1], WU Mingfang[1], CENG Yue[2], WANG Huan[2], SHEN Songpei[2] (1. Jiang Su university of science and technology, Jiang Su, Zhenjiang 212003, China; 2. HuDong-ZhongHua Ship Building Company Limited, Shanghai 200129, China). pp 45 – 48

Abstract: Using the three-dimensional finite element method, the residual deformation of joints obtained with the AH36 steel plate with thickness of 6 mm under different welding conditions was studied in this paper. The numerical simulation results showed that the longitudinal distortion and the angular distortion changed dramatically. As to different welding methods, the deformation was small when the unique CO_2 gas arc welding was used, while large deformation was found when the CO_2 arc and SAW were combined together. The residual deformation was controlled effectively by water cooling, especially for angular deformation with the unique CO_2 gas arc welding. To verify the finite element simulation results, an experiment using the same parameters was done. With some error, the experimental results were consistent with the numerical results, indicating that the welding deformation in different welding conditions can be simulated with the three-dimensional finite element method.

Key words: marine steel plate; residual deformation; water cooling; finite element modeling

Interfacial microstructure and properties of SnCuNi-*x*Pr/Cu solder joint LUO Jiadong[1], XUE Songbai[1], YE Huan[1], YANG Jingqiu[2] (1. College of Materials Science and Technology, Nanjing University of Aeronautics and Astronautics, Nanjing 210016, China; 2. Harbin Welding Institute, Harbin 150080, China). pp 49 – 52

Abstract: Effects of rare earth element Pr on the intermetallics (ZMC) between Sn0.7Cu0.05Ni-xPr lead-free solder and Cu substrate were studied in this paper. And the possible influence mechanism was initially introduced. The experimental results showed that the interface morphology was greatly modified and became more uniform and flat due to the addition of Pr, and the effect of 0.05% Pr addition was more remarkable than that of 0.15% Pr. Adding Pr could reduce the driving force and time of the interfacial reaction to restrain excessive IMC growth. It was concluded that there was a synergistic effect on the interfacial reaction between Pr and Ni. The strength and ductility of the solder joint were greatly improved due to the refined microstructure because of the pinning effect on the migration of grain boundaries brought by adding Pr, and precipitation hardening strengthened